Co-optimizing Behind-The-Meter Resources under Net Metering

Ahmed S. Alahmed and Lang Tong ({asa278, lt35}@cornell.edu)
School of Electrical and Computer Engineering, Cornell University, Ithaca, USA

2023 IEEE Texas Power and Energy Conference (TPEC) | 978-1-6654-9071-9/23/$31.00 ©2023 IEEE | DOI: 10.1109/TPEC56611.2023.10078677

***Abstract*—We study the problem of co-optimizing behind-the-meter (BTM) storage and flexible demands with BTM stochastic renewable generation. Under a generalized net energy metering (NEM) policy—NEM X, we show that the optimal co-optimization policy schedules the flexible demands based on a priority list that defers less important loads to times when the BTM generation is abundant. This gives rise to the notion of a net-zero zone, which we quantify under different distributed energy resources (DER) compositions. We highlight the special case of inflexible demands that results in a storage policy that minimizes the imports and exports from and to the grid. Comparative statics are provided on the optimal co-optimization policy. Simulations using real residential data show the surplus gains of various customers under different DER compositions.**

***Index Terms*—demand response, distributed energy resources, energy storage, home energy management, net metering.**

I. Introduction

The falling prices of battery storage and the unremitting reduction of NEM compensation rates for grid exports ushered storage deployment in residential households, especially those coupled with rooftop solar[1]. The increasing differential between the rates of energy imports and exports under NEM, increases the value of self-consuming the BTM generation, which can be achieved by demand response [3], energy storage [4], or both [5].

Substantial research studied energy management systems (EMS) under the existence of DER. The work in [5], however, was the first to propose a linear-complexity and near closed-form characterization to the storage and flexible loads co-optimization, which enables scheduling massive numbers of such resources as functions of the BTM renewable distributed generation (DG). In this work, we expand on the analysis in [5] by deriving additional structural properties and special cases that give more insights to the optimal co-optimization policy.

The optimization of BTM storage operation has been extensively studied. Researchers have studied the optimal operation of storage for various objectives including bill minimization (or surplus maximization) [6]–[8], wholesale market participation [9], and grid services provision [10]. The literature on BTM residential storage operation largely omitted the situation of dynamically controlling both the household's consumption and storage to maximize the customer's benefit by actively scheduling the resources as functions of the renewable DG. The handful of work done on consumption and storage co-optimization either lacks the analyticity of our proposed solution [6], [9], [11], or co-optimizes storage and time-of-service of deferrable load [7], [8] rather than the quantity of the elastic load, as presented in our work.

This work builds upon the optimal policy derived in [5], which co-optimizes flexible loads and energy storage under the existence of stochastic renewable generation when prosumers (customers with DG or storage) face NEM X tariff, by providing insights, interpretations, and special cases to the solution structure. To this end, four results are presented. First, we show that the optimal policy generates a load priority list that schedules demands based on the DG profile. Second, we prove that the special case of inflexible demands simplifies the optimal policy to one that minimizes prosumer's imports and exports from and to the grid. Third, we quantify the net-zero zone, where the prosumer is operationally off-the-grid, under different DER compositions. Lastly, we perform comparative statics on the co-optimization policy's optimal decisions

Our simulation results adopt the Californian NEM 3.0 policy (also called *net billing*) to model household's payment, under various customers types, including those with and without storage, DG and flexible demands. The surplus gain and percentage of self-consumed DG of the different customer types are investigated while varying tariff and storage parameters.

II. Problem Formulation and Optimal Decisions

We consider a household with BTM DER, including flexible demands, a renewable DG, and an energy storage, facing an electric utility under NEM (Fig.1). The surplus-maximizing household co-optimizes its BTM DER, which reveals appealing decision and operational structures that we investigate.

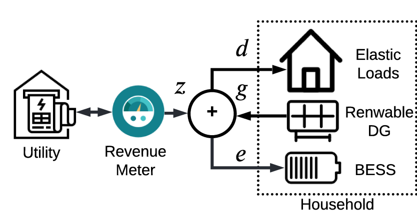

Fig. 1. Solar+storage prosumer under NEM. The variables of load consumption d and DG output g are real and non-negative, whereas storage output e and net consumption z variables are real.

This work was supported in part by the National Science Foundation under Grants 1932501 and 2218110.

The full paper, including proofs of theoretical results, is available at [1].

[1]According to [2], the total installed BTM storage capacity in 2020 reached 1000 MW, and 80% of the residential storage capacity is paired with solar.

A. BTM DER Models

We study the sequential scheduling of consumption $(\mathbf{d}_t)$ and battery operation (e_t) of the arrangement in Fig.1 over a finite horizon indexed by $t = 0, \ldots, T-1$.

a) Flexible demand: The prosumer has K devices whose consumption vector, for every $t = 0, \ldots, T-1$, is denoted by $\boldsymbol{d}_t = (d_{t1}, \cdots, d_{tK}) \in \mathcal{D}$, with

$$\mathcal{D} := \{\boldsymbol{d} : \underline{\boldsymbol{d}} \preceq \boldsymbol{d} \preceq \overline{\boldsymbol{d}}\} \subseteq \mathbb{R}_+^K,$$

where $\underline{\boldsymbol{d}}, \overline{\boldsymbol{d}}$ represent the consumption's lower and upper bounds, respectively.

The utility $U_t(\mathbf{d}_t)$ of consuming $\mathbf{d}_t$ in interval t is assumed to be strictly concave, strictly increasing, continuously differentiable, and additive, i.e.,

$$U_t(\mathbf{d}_t) := \sum_{k=1}^{K} U_{tk}(d_{tk}), \quad t = 0, \ldots, T-1. \tag{1}$$

The marginal utility function is denoted and defined by

$$\mathbf{L}_t := \nabla U_t = (L_{t1}, \cdots, L_{tK}). \tag{2}$$

b) Renewable: For $t = 0, \ldots, T-1$, the *DG output* $g_t \in \mathbb{R}_+$ is an exogenous (positive) Markovian random process.

c) Battery storage: For $t = 0, \ldots, T-1$, the *battery control* is given by $e_t = [e_t]^+ - [e_t]^- \in [-\underline{e}, \bar{e}]$, where $[x]^+ := \max\{0, x\}$ and $[x]^- := -\min\{0, x\}$ denote the positive and negative part functions for any $x \in \mathbb{R}$, respectively, and $\underline{e}$ and $\bar{e}$ are the limits of battery's discharging and charging rates, respectively. When $e_t > 0$, the storage is charged, and when $e_t < 0$, the storage is discharged.

The efficiencies of discharging and charging the storage are denoted by $\rho, \tau \in (0, 1]$, respectively. This means that charging with $[e_t]^+$ increases the SoC by $\tau[e_t]^+$, whereas discharging by $[e_t]^-$ decreases the SoC by $\frac{1}{\rho}[e_t]^-$. We denote the storage SoC by $s_t \in [\underline{s}, \bar{s}]$ with $\underline{s}$ and $\bar{s}$ as the lower and upper SoC bounds, respectively. The SoC evolution is driven by e_t as

$$s_{t+1} = s_t + \tau[e_t]^+ - [e_t]^-/\rho, \quad t = 0, \ldots, T-1, \tag{3}$$

with $s_0 = s$ as the initial SoC, which is assumed to be exogenous and independent of the household's decisions.

B. NEM X Tariff Model

The customer's payment to the utility under NEM policy is based on the household's *net-consumption* $z_t \in \mathbb{R}$ defined by

$$z_t := \mathbf{1}^\top \boldsymbol{d}_t + e_t - g_t, \quad t = 0, \ldots, T-1. \tag{4}$$

The period at which the netting operation under NEM is performed might be as brief as 5 minutes and as extended as a month [12]. For brevity, we limit our exposition to the instance when the NEM netting period is equivalent to the prosumer scheduling period, allowing us to index the netting period by t as well.

By adopting the NEM X tariff model introduced in [3], we use the NEM X tariff parameter $\pi_t = (\pi_t^+, \pi_t^-, \pi_t^0)$, to compute the household's *payment* (bill) under NEM X as

$$P_t^{\pi_t}(z_t) := \pi_t^+[z_t]^+ - \pi_t^-[z_t]^- + \pi_t^0, \quad t = 0, \ldots, T-1, \tag{5}$$

where $\pi_t^+, \pi_t^-, \pi_t^0 \in \mathbb{R}_+$ are the *retail (buy) rate*, *export (compensation) rate*, and *fixed (connection) charge*[2], respectively. For every $t = 0, \ldots, T-1$, when $z_t \geq 0$, the prosumer is a *net-consumer* facing π_t^+, whereas when $z_t < 0$, the prosumer is a *net-producer* facing π_t^-.

The retail and export rates can be temporally varying (e.g., time-of-use (ToU)) or fixed (e.g., flat pricing).

C. Prosumer Decision Problem

The problem is formulated as a T-stage Markov decision process (MDP). The MDP state in interval t consists of storage SoC s_t and renewable DG output g_t, $x_t := (s_t, g_t) \in \mathcal{X}$. The evolution of the MDP state is defined by (3) and the exogenous Markov random process (g_t). The MDP initial state is denoted by $x_0 = (s, g)$.

The MDP *policy* $\mu := (\mu_0, \ldots, \mu_{T-1})$ is a sequence of decision rules, $x_t \xrightarrow{\mu_t} u_t := (\boldsymbol{d}_t, e_t)$, for all x_t and t, that determines consumption and battery schedule in each stage. The reward function $r_t^{\pi_t}$ consists of *prosumer surplus* $S_t^{\pi_t}$ as a stage reward, and *storage salvage value* as a terminal reward:

$$r_t^{\pi_t}(x_t, u_t) := \begin{cases} S_t^{\pi_t}(u_t; g_t), & t \in [0, T-1] \\ \gamma(s_T - s), & t = T, \end{cases} \tag{6}$$

where

$$S_t^{\pi_t}(u_t; g_t) := U_t(\boldsymbol{d}_t) - P_t^{\pi_t}(\mathbf{1}^\top \boldsymbol{d}_t - g_t + e_t), \tag{7}$$

and γ is the salvage value of stored energy.

The storage and flexible loads co-optimization is given by

$$\begin{aligned}
\mathcal{P} : \underset{\mu=(\mu_0,\ldots,\mu_{T-1})}{\text{Maximize}} \quad & \mathbb{E}_\mu \left\{ \sum_{t=0}^{T} r_t^{\pi_t}(x_t, u_t) \right\} && \text{(8a)} \\
\text{Subject to} \quad & \text{for all } t = 0, \ldots, T-1, \\
& s_{t+1} = s_t + \tau[e_t]^+ - [e_t]^-/\rho && \text{(8b)} \\
& g_{t+1} \sim F_{g_{t+1}|g_t} && \text{(8c)} \\
& \underline{s} \leq s_t \leq \bar{s} && \text{(8d)} \\
& 0 \leq [e_t]^- \leq \underline{e} && \text{(8e)} \\
& 0 \leq [e_t]^+ \leq \bar{e} && \text{(8f)} \\
& \underline{\boldsymbol{d}} \preceq \boldsymbol{d}_t \preceq \overline{\boldsymbol{d}} && \text{(8g)} \\
& x_0 = (s, g), && \text{(8h)}
\end{aligned}$$

where the expectation is over the exogenous stochastic renewable generation (g_t), and $F_{g_{t+1}|g_t}$ is the conditional distribution of g_{t+1} given g_t.

D. Optimal Prosumer Decisions

The solution of the storage-consumption co-optimization in (8) is provided in [5] under two assumptions: (A1) non-binding SoC limits (8d), and (A2) sandwiched salvage value, where

$$\max\{(\pi_t^-)\} \leq \tau\gamma \leq \gamma/\rho \leq \min\{(\pi_t^+)\}. \tag{9}$$

Under A1-A2, the solution has a highly-scalable threshold-based structure that co-schedules the consumption and storage

[2]Without loss of generality, we assume zero fixed charges ($\pi_t^0 = 0, \forall t$), as the optimization and solution structure are not affected by it.

based on the availability and level of the BTM DG. For every $t = 0, \ldots, T-1$, the co-optimization policy has six BTM-DG-independent thresholds, ordered as

$$\Delta_t^- \geq \sigma_t^- \geq \sigma_t^{-o} \geq \sigma_t^{+o} \geq \sigma_t^+ \geq \Delta_t^+, \tag{10}$$

and computed as:

$$\begin{array}{lll} \Delta_t^+ := f_t(\pi_t^+) - \underline{e}, & \sigma_t^+ := f_t(\gamma/\rho) - \underline{e}, & \sigma_t^{+o} := f_t(\gamma/\rho) \\ \Delta_t^- := f_t(\pi_t^-) + \overline{e}, & \sigma_t^- := f_t(\tau\gamma) + \overline{e}, & \sigma_t^{-o} := f_t(\tau\gamma) \end{array} \tag{11}$$

where f_t is the sum of inverse marginal utilities defined as

$$f_t(\pi_t) := \sum_{k=1}^{K} f_{tk}(\pi_t) \tag{12}$$

$$f_{tk}(\pi_t) := \max\{\underline{d}_k, \min\{L_{tk}^{-1}(\pi_t), \overline{d}_k\}\}, \tag{13}$$

and L_{tk} is as defined in (2) with L_{tk}^{-1} as its inverse.

For every $t = 0, \ldots, T-1$, the *optimal consumption* $d_{tk}^*(g_t)$ of every device k, *battery operation* $e_t^*(g_t)$, *net-consumption* $z_t^*(g_t)$, and the resulting payment $P_t^{*,\pi_t}(g_t)$ are monotonic in g_t, and their structures are summarized in Table I (Also depicted in Fig.3). The household operates in 1) the net consumption zone $(+)$ if $g_t \leq \Delta_t^+$, 2) the net production zone $(-)$ if $g_t \geq \Delta_t^-$, and 3) the net zero zone (0) if $g_t \in [\Delta_t^+, \Delta_t^-]$, under which the household is off-the-grid.

III. Solution Properties and Special Cases

We discuss some properties and special cases of the optimal co-optimization policy in Sec.II-D. Sec.III-A shows the load priority ranking structure of the solution. Sec.III-B considers the special case of solving (8) under passive[3] demands. Sec.III-C, quantifies the net zero zone, and show that the more flexible resources the prosumer has, the larger its net zero zone. Lastly, Sec.III-D, provides comparative statics analysis on the solution structure.

A. Load Priority Ranking Rule

The optimal consumption schedule reveals important microeconomics interpretations based on marginal utilities of devices and the rates $\pi_t^+, \pi_t^-, \gamma/\rho$ and $\tau\gamma$. Devices with higher marginal utilities are prioritized in the net-consumption zone $(z_t^*(g_t) > 0)$; when the DG output is low. Less important devices (lower marginal utilities) are exercised only when the DG output is high. Proposition 1 formalizes the conditions for device consumptions in each net-consumption zone.

Proposition 1 (Load priority ranking rule)**.** *Under A1-A2, and assuming w.l.o.g that* $\underline{d}_k = 0, \forall k$*, the scheduling of every device* k *and* $t = 0, \ldots, T-1$ *in any of the three consumption zones, depends on its marginal utility* $L_{tk}(\cdot)$*. If*

1) $L_{tk}(0) > \pi_t^+$*, device* k *is consumed in all zones.*
2) $\pi_t^+ \geq L_{tk}(0) > \gamma/\rho$*, device* k *is consumed in all zones, except the net-consumption zone.*
3) $\gamma/\rho \geq L_{tk}(0) > \tau\gamma$*, device* k *is consumed only if* $g_t > \sigma_t^{+o}$.
4) $\tau\gamma \geq L_{tk}(0) > \pi_t^-$*, device* k *is consumed only if* $g_t > \sigma_t^-$.
5) $\pi_t^- > L_{tk}(0)$*, device* k *is never consumed.* □

[3]We use *passive* and *active* to refer to customers with DG-inelastic and DG-elastic demands, respectively [12].

To illustrate Proposition 1, marginal utilities of five devices corresponding to the 5 cases in Proposition 1 are shown in Fig.2. Note that since the marginal utility of device 1 at zero consumption $L_{t1}(0)$ is greater than π_t^+, the device was consumed in all zones because the non-increasing marginal utility intersected all of the four price lines, granting a positive consumption. On the other hand, for device 55, since $(L_{t5}(0) \leq \pi_t^-)$, the device was not consumed in any zone. Devices 2, 3 and 4 do not consume in the net-consumption zone since $L_{t2}(0), L_{t3}(0), L_{t4}(0) < \pi_t^+$, however, they start consuming from the smallest point under which their marginal utilities intersect with the price.

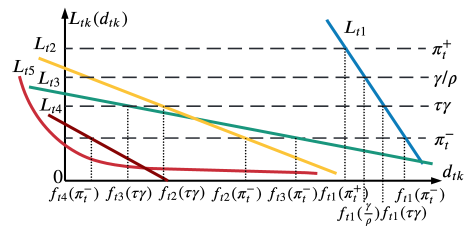

Fig. 2. Consumption allocation to devices based on marginal utilities.

B. Passive Prosumer

For every $t = 0, \ldots, T-1$, the *passive SDG*[4] prosumer schedules the consumption as if the household faces only π_t^+, and therefore consumes $f_t(\pi_t^+)$ for any DG output. It turns out that the the optimal policy of a passive SDG prosumer is to minimize the absolute value of its net-consumption z_t.

Proposition 2 (Optimal policy under DG-passive demands)**.** *Under A1-A2 and for any DG-passive consumption bundle* $\hat{\boldsymbol{d}}_t \in \mathcal{D}$*, the optimal storage operation is to discharge/charge as much as possible to minimize the absolute value of net consumption:*

$$\mu_t^* \in \underset{e_t \in \{-\underline{e}, \overline{e}\}}{\text{arg min}} \quad |z_t|. \tag{14}$$

for every $t = 0, \ldots, T-1$, □

The passive SDG prosumer optimal policy is intuitive (Fig.3). The storage exercises a *balancing control* that tries to null the renewable-adjusted consumption $\tilde{d}_t := \mathbf{1}^\top \hat{\boldsymbol{d}}_t - g_t$ [13]. For the given fixed total consumption $f_t(\pi_t^+)$, the battery's stored energy is used to a) reduce net consumption in case $\tilde{d}_t < 0$, b) increase net consumption (production) in case $\tilde{d}_t > 0$, and c) maintain net-zero as much as possible. Under (a), the prosumer gains at the rate of π^+ and losses at the rate of γ/ρ, whereas under (b), the prosumer gains at the rate of $\tau\gamma$ and losses at the rate of π^-. Proposition 2 also implies

[4]We refer to prosumers with standalone DG as *DG prosumers*, and prosumers with storage and DG as *SDG prosumers*.

TABLE I
SUMMARY OF THE OPTIMAL CO-OPTIMIZATION POLICY.

Zone	$(+)$	(0)					$(-)$
g_t	$g_t < \Delta^+$	$g_t \in (\Delta_t^+, \sigma_t^+]$	$g_t \in (\sigma_t^+, \sigma_t^{+o}]$	$g_t \in (\sigma_t^{+o}, \sigma_t^{-o}]$	$g_t \in (\sigma_t^{-o}, \sigma_t^-]$	$g_t \in (\sigma_t^-, \Delta_t^-]$	$g_t > \Delta_t^-$
$d_{tk}^*(g_t)$	$f_{tk}(\pi_t^+)$	$f_{tk}(f_t^{-1}(g_t + \underline{e}))$	$f_{tk}(f_t^{-1}(\gamma/\rho))$	$f_{tk}(f_t^{-1}(g_t))$	$f_{tk}(f_t^{-1}(\gamma\tau))$	$f_{tk}(f_t^{-1}(g_t - \overline{e}))$	$f_{tk}(\pi_t^-)$
$e_t^*(g_t)$	$-\underline{e}$	$-\underline{e}$	$g_t - \sigma_t^{+o}$	0	$g_t - \sigma_t^{-o}$	$\overline{e}$	$\overline{e}$
$z_t^*(g_t)$	$z_t^* > 0$	$z_t^* = 0$	$z_t^* = 0$	$z_t^* = 0$	$z_t^* = 0$	$z_t^* = 0$	$z_t^* < 0$
$P_t^{*,\pi_t}(g_t)$	$\pi_t^+ z_t^*$	0	0	0	0	0	$\pi_t^- z_t^*$

that the ratio of self-consumption over the scheduling period $SC \in [0, 1]$, defined by

$$SC(z_t) := 1 + \sum_{t=0}^{T-1} \frac{[z_t]^-}{g_t}, \text{ for } \sum_{t=0}^{T-1} g_t > 0, \tag{15}$$

is maximized.

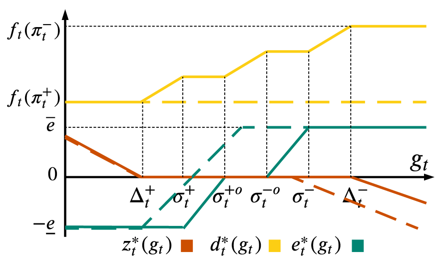

Fig. 3. Active (solid) and passive (dashed) SDG prosumers decisions.

C. Net Zero Zone Quantification

The *passive SDG* prosumer case shows the propensity of prosumers to achieve net-zero. We hence define and quantify the net-zero zone length under different DER compositions.

Definition 1 (Net-zero zone length)**.** *For $t = 0, \ldots, T-1$, and for any optimal policy $\boldsymbol{\mu}^*$ the net-zero zone length is given by*

$$|\mathcal{G}_t^{\boldsymbol{\mu}^*}| := \underset{g_t \in \mathcal{G}_t^{\boldsymbol{\mu}^*}}{\text{Maximize}}\ g_t - \underset{g_t \in \mathcal{G}_t^{\boldsymbol{\mu}^*}}{\text{Minimize}}\ g_t \tag{16}$$

where $\mathcal{G}_t^{\boldsymbol{\mu}^*} = \{g_t \in \mathbb{R}_+ : z_t^{\boldsymbol{\mu}^*}(g_t) = 0\}$ is a convex set.

Definition 1 is used in Corollary 1 to show that the co-optimization policy's net-zero zone length is the sum of the net-zero zone lengths of *DG active* [3] and *SDG passive* prosumers (Sec.III-B).

Corollary 1 (Net-zero zone length quantification)**.** *Under A1-A2, and for every $t = 0, \ldots, T-1$, the net-zero zone lengths of optimal: 1) passive DG $|\mathcal{G}_t^{\boldsymbol{\mu}_1^*}|$, 2) active DG $|\mathcal{G}_t^{\boldsymbol{\mu}_2^*}|$, 3) passive SDG $|\mathcal{G}_t^{\boldsymbol{\mu}_3^*}|$ and 4) active SDG $|\mathcal{G}_t^{\boldsymbol{\mu}_4^*}|$ prosumers are ordered as*

$$|\mathcal{G}_t^{\boldsymbol{\mu}_4^*}| \geq |\mathcal{G}_t^{\boldsymbol{\mu}_3^*}| \geq |\mathcal{G}_t^{\boldsymbol{\mu}_2^*}| \geq |\mathcal{G}_t^{\boldsymbol{\mu}_1^*}|, \tag{17}$$

if $f_t(\pi_t^-) - f_t(\pi_t^+) \leq \overline{e} + \underline{e}$, and ordered as

$$|\mathcal{G}_t^{\boldsymbol{\mu}_4^*}| \geq |\mathcal{G}_t^{\boldsymbol{\mu}_2^*}| \geq |\mathcal{G}_t^{\boldsymbol{\mu}_3^*}| \geq |\mathcal{G}_t^{\boldsymbol{\mu}_1^*}|, \tag{18}$$

if $f_t(\pi_t^-) - f_t(\pi_t^+) > \overline{e} + \underline{e}$.

It also holds that

$$|\mathcal{G}_t^{\boldsymbol{\mu}_4^*}| = |\mathcal{G}_t^{\boldsymbol{\mu}_2^*}| + |\mathcal{G}_t^{\boldsymbol{\mu}_3^*}|. \tag{19}$$

□

The corollary shows that the more flexible resources (active loads and storage) an optimal prosumer has, the longer its net-zero zone length, as in $|\mathcal{G}_t^{\boldsymbol{\mu}_4^*}|$. The length of net-zero zone is compromised if one or both of the decision variables are dropped, i.e., $\boldsymbol{d}$ in $|\mathcal{G}_t^{\boldsymbol{\mu}_3^*}|$, e in $|\mathcal{G}_t^{\boldsymbol{\mu}_2^*}|$ and both $\boldsymbol{d}, e$ in $|\mathcal{G}_t^{\boldsymbol{\mu}_1^*}|$.

Shrinking the net-production and net-consumption zones lengths, while increasing $|\mathcal{G}_t^{\boldsymbol{\mu}^*}|$ has crucial economical and technical implications. As $|\mathcal{G}_t^{\boldsymbol{\mu}^*}|$ increases, the customer's bill becomes more immune to π^- reductions, because SC in (15) becomes higher. For grid operators and utilities, higher $|\mathcal{G}_t^{\boldsymbol{\mu}^*}|$ achieves operational benefits such as reducing reverse power flows, which improves network's reliability [14]. This, however, may come at the cost of higher grid defection rates [15], requiring utilities to reshape their business model.

D. Comparative Statics

Here we offer a comparative statics analysis on the optimal policy to investigate how the parameters and variables influence the solution structure in each net-consumption zone. Theorem 1 in [1] formalizes the effect of changing exogenous parameters on the endogenous quantities of consumption, storage operation, payment, and surplus. Table II summarizes the comparative static analysis by considering ϵ-increases of the exogenous parameters and examining changes of endogenous quantities at interior points of the three zones.

Table II shows that the increase in the renewable output enables increasing the consumption and the storage output, which results in a decreasing payment and increasing surplus. This is because, under NEM X, self-consumption of the renewable output is valued more than exporting it back.

Varying the NEM X tariff parameters $\pi = (\pi^+, \pi^-, \pi^0)$, as shown in Table II have direct implication on $S_t^{*,\pi_t}(g_t)$. Increasing π_t^+ negatively affects $S_t^{*,\pi_t}(g_t)$, since the household consumption will be reduced. However, increasing the export rate positively effect $S_t^{*,\pi_t}(g_t)$ as the payment to the utility reduces and the consumption increases. Increasing π_t^0 reduces $S_t^{*,\pi_t}(g_t)$, because the payment increases. Interestingly, the storage output is independent of the NEM X tariff parameters.

The salvage value rate affects the optimal consumption, storage operation, and prosumer surplus only in the net-zero zone, where the consumption and surplus reduce as γ increases, and the storage output increases as γ increases.

TABLE II
COMPARATIVE STATIC ANALYSIS.

Quantity	Zone	$g_t \uparrow$	$\pi_t^+ \uparrow$	$\pi_t^- \uparrow$	$\gamma \uparrow$	$\pi_t^0 \uparrow$
$d_{tk}^*(g_t)$	+	—	↓	—	—	—
	−	—	—	↓	—	—
	0	↑	—	—	↓	—
$e_t^*(g_t)$	+	—	—	—	—	—
	−	—	—	—	—	—
	0	↑	—	—	↑	—
$P_t^{*,\pi_t}(g_t)$	+	↓	×	—	—	↑
	−	↓	—	↓	—	↑
	0	—	—	—	—	↑
$S_t^{*,\pi_t}(g_t)$	+	↑	↓	—	—	↓
	−	↑	—	↑	—	↓
	0	↑	—	—	↓	↓

↑ : increasing ↓ : decreasing — : unchanged × : indeterminant

IV. NUMERICAL RESULTS

We consider a household receiving service under a NEM policy. Five prosumer types are studied: 1) *consumers*: customers without BTM DER, 2) *active DG prosumers*: customers who schedule their consumption based on available DG [3], 3) *active SDG prosumers*[5]: customers who co-optimize storage and consumption as in Sec.II-D, 4) *passive DG* and 5) *passive SDG prosumers*: customers who do not schedule consumption based on available DG. *Passive prosumers* consume as if they are *consumers*.

To model household consumption and renewable generation, we used the Smart project data set[6], which has a 1-minute granularity of aggregated and individual home circuits collected over the year 2016. We restricted our simulation to only three months of 2016 (June-August).

The consumption preferences are captured by the following, widely-adopted, quadratic concave utility function

$$U_{tk}(d_{tk}) = \begin{cases} \alpha_{tk} d_{tk} - \frac{\beta_{tk}}{2} d_{tk}^2, & 0 \leq d_{tk} < \frac{\alpha_{tk}}{\beta_{tk}} \\ \frac{\alpha_{tk}^2}{2\beta_{tk}}, & d_{tk} \geq \frac{\alpha_{tk}}{\beta_{tk}}, \end{cases} \tag{20}$$

where α_{tk} and β_{tk} are some utility parameters that are learned using historical consumption and price data by positing an elasticity of demand[7] as in [12].

The discharging and charging efficiencies of the battery ρ, τ were assumed to be 0.95. By considering Tesla Powerwall[8] 2, the capacity of the battery was chosen to be 13.5 kWh. The salvage value γ was chosen such that A2 in (9) holds.

The household faces the Californian NEM 3.0 tariff, which has a ToU-based retail rate π^+, a dynamic avoided-cost-based export rate π^-, and a fixed charge of $\pi^0 = \$15$/month. For π^+, we adopted PG&E 2022 summer E-TOU-B rate schedule, which has peak and off-peak rates of $\pi_h^+ = \$0.49$/kWh and $\pi_l^+ = \$0.37$/kWh, respectively, and a 16–21 peak period. For π^-, the 2022 average avoided cost rates, developed by E3 Inc. avoided cost calculator (ACC), were used[9].

A. Surplus Gain

We compared the average daily surplus gain achieved by the five prosumer types, using *consumers* as the benchmark. Table III shows the average percentage gain in daily surplus over that achieved by a *consumer* under one-minute and one-hour netting frequencies and three different storage charge/discharge rates $\overline{e} = \underline{e} \in \{0.5, 0.75, 1\}$.

Four key observations are in order. First, *active SDG* customers achieved the highest surplus gain of all cases. Second, increasing the netting frequency from an hourly to a minute basis always resulted in lower surplus gains, as customers became more vulnerable to the lower export rate. Third, the value of being *active* was significant, with an 8% surplus gain increase for both *DG* and *SDG* customers. Lastly, increasing the storage rate by 0.25kW for both *passive* and *active* customers resulted in a roughly 4% surplus gain.

TABLE III
SURPLUS GAIN OVER CONSUMERS (%).

DER	Customer	$\overline{e} = \underline{e}$ (kW)	1-min	1-hour
–	Consumer	0	0	0
DG	Passive	0	69.27	70.82
	Active	0	77.48	79.21
DG + Storage	Passive	0.5	81.27	82.98
		0.75	86.13	87.90
		1	90.52	92.33
	Active	0.5	89.44	91.23
		0.75	94.19	96.02
		1	98.32	100.25

B. DG Self-Consumption

Table IV shows the self-consumption (computed as in (15)) percentage of the studied customer types under a one-minute and one-hour netting frequencies and three different storage charge/discharge rates $\overline{e} = \underline{e} \in \{0.5, 0.75, 1\}$.

Broadly speaking, customers who achieved high surplus gains in Table III managed to achieve high self-consumption percentages (Table IV). This is, however, not always the case, as *active DG* prosumers achieved higher self-consumption but lower surplus gain compared to *passive SDG* prosumers with 0.5kW storage charge/discharge rates. The reason is that, although *active DG* prosumers more effectively reduced energy exports, they under-performed in reducing energy imports compared to *SDG* prosumers, which is more costly. At 0.75kW and 1kW storage rates, *passive SDG* prosumers had both higher surplus gains and higher self-consumption.

Table IV shows that increasing the netting frequency decreased the self-consumption percentage, as customers had a shorter banking period for loads to consume the DG output. For both netting frequencies, installing a DG without actively

[5]SDG prosumers are customers with storage+DG.

[6]The data repository can be accessed at Smart Data Set. We used home D.

[7]The long-run price elasticity of electricity demand used was -0.21 [16].

[8]Tesla Powerwall datasheet can be found at Tesla Powerwall.

[9]The ACC rates can be accessed at E3 ACC.

scheduling the consumption based on the available DG, resulted in exporting back more than 57% of the DG. Actively scheduling the consumption based on the available DG, as proposed [3], increased self-consumption to over 55%. When the prosumer installed storage in addition to the DG, self-consumption increased to more than 61% when the customer was *passive*, and to over 74% when the prosumer was *active*.

TABLE IV
DG SELF-CONSUMPTION (%).

DER	Customer	$\overline{e} = \underline{e}$ (kW)	1-min	1-hour
–	Consumer	0	–	–
DG	Passive	0	41.02	42.25
	Active	0	55.22	56.68
DG + Storage	Passive	0.5	52.22	53.32
		0.75	57.18	58.19
		1	61.64	62.67
	Active	0.5	66.24	67.40
		0.75	70.87	71.97
		1	74.79	76.00

C. Value of Storage

Fig.4, shows surplus gains of *active* and *passive SDG* prosumers compared to *active* and *passive DG* prosumers[10] under varying export rates (left) and storage efficiencies (right).

The left plot shows that the value of storage (VoS) and the value of demand response (VDR) increased as the differential between the retail and export rates enlarged. The gain increase was higher in the *active SDG – passive DG* case (yellow) because the curve augmented both VDR and VoS. The surplus gain increased in the *passive SDG – passive DG* (orange) and *active SDG – active DG* (blue) cases, as the π^- decreased was primarily due to VoS, which has a higher value when locally absorbing g becomes more valuable. The *passive SDG – active DG* surplus gain as π^- decreased, compares the effectivity of VoS alone and VDR alone in reducing exported generation.

The right plot shows that VoS increased as the storage charging/discharging efficiencies increased. Interestingly, the *passive SDG – active DG* curve (purple) shows that when the storage was relatively inefficient, VDR exceeded VoS, which was reversed as the storage efficiency improved.

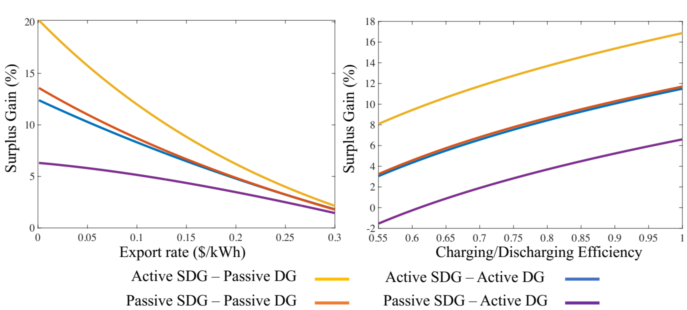

Fig. 4. Surplus gain over active/passive DG prosumers ($\overline{e} = \underline{e} = 0.75$kW).

[10]This is also called *value of storage*.

V. CONCLUSION

This work analyzed the structural properties of the optimal policy co-optimizing flexible demands and storage devices when operated with a renewable DG. The policy is shown to abide by a load priority ranking rule that exercises consumption decisions based on load importance, which gets relaxed when the renewables are abundant. Comparative statics on the optimal decisions, prosumer payment, and reward have been investigated under different tariff and household DER parameters. Lastly, it has been shown that under the special case of inflexible demands, the storage is operated in a manner that minimizes the inflows and outflows from and to the grid.

REFERENCES

[1] A. S. Alahmed and L. Tong, "Co-optimizing behind-the-meter resources under net metering," 2022. [Online]. Available: https://arxiv.org/abs/2212.03311

[2] G. L. Barbose, S. Elmallah, and W. Gorman, "Behind the meter solar+storage: Market data and trends," Lawrence Berkeley National Laboratory, Tech. Rep., 07 2021.

[3] A. S. Alahmed and L. Tong, "On net energy metering X: Optimal prosumer decisions, social welfare, and cross-subsidies," *IEEE Transactions on Smart Grid*, pp. 1–1, 2022.

[4] N. R. Darghouth, G. L. Barbose, and A. D. Mills, "Implications of rate design for the customer-economics of behind-the-meter storage," Lawrence Berkeley National Laboratory, Tech. Rep., 08 2019. [Online]. Available: https://emp.lbl.gov/webinar/implications-rate-design-customer

[5] A. S. Alahmed, L. Tong, and Q. Zhao, "Co-optimizing distributed energy resources in linear complexity under net energy metering," 2022. [Online]. Available: https://arxiv.org/abs/2208.09781

[6] M. A. A. Pedrasa, T. D. Spooner, and I. F. MacGill, "Coordinated scheduling of residential distributed energy resources to optimize smart home energy services," *IEEE Transactions on Smart Grid*, vol. 1, no. 2, pp. 134–143, 2010.

[7] Y. Xu and L. Tong, "Optimal operation and economic value of energy storage at consumer locations," *IEEE Transactions on Automatic Control*, vol. 62, no. 2, pp. 792–807, 2017.

[8] Y. Guo, M. Pan, Y. Fang, and P. P. Khargonekar, "Decentralized coordination of energy utilization for residential households in the smart grid," *IEEE Transactions on Smart Grid*, vol. 4, no. 3, 2013.

[9] J. Garcia-Gonzalez, R. M. R. de la Muela, L. M. Santos, and A. M. Gonzalez, "Stochastic joint optimization of wind generation and pumped-storage units in an electricity market," *IEEE Transactions on Power Systems*, vol. 23, no. 2, pp. 460–468, 2008.

[10] H. Hao, D. Wu, J. Lian, and T. Yang, "Optimal coordination of building loads and energy storage for power grid and end user services," *IEEE Transactions on Smart Grid*, vol. 9, no. 5, pp. 4335–4345, 2018.

[11] N. Li, L. Chen, and S. H. Low, "Optimal demand response based on utility maximization in power networks," in *2011 IEEE Power and Energy Society General Meeting*, 2011, pp. 1–8.

[12] A. S. Alahmed and L. Tong, "Integrating distributed energy resources: Optimal prosumer decisions and impacts of net metering tariffs," *SIGENERGY Energy Inform. Rev.*, vol. 2, no. 2, p. 13–31, Aug. 2022. [Online]. Available: https://doi.org/10.1145/3555006.3555008

[13] P. Harsha and M. Dahleh, "Optimal management and sizing of energy storage under dynamic pricing for the efficient integration of renewable energy," *IEEE Transactions on Power Systems*, vol. 30, no. 3, pp. 1164–1181, 2015.

[14] E. L. Ratnam, S. R. Weller, and C. M. Kellett, "Scheduling residential battery storage with solar PV: Assessing the benefits of net metering," *Applied Energy*, vol. 155, pp. 881–891, 2015.

[15] S. Borenstein, "Can net metering reform fix the rooftop solar cost shift?" Jan. 2021. [Online]. Available: https://energyathaas.wordpress.com

[16] A. Asadinejad, A. Rahimpour, K. Tomsovic, H. Qi, and C. fei Chen, "Evaluation of residential customer elasticity for incentive based demand response programs," *Electric Power Systems Research*, vol. 158, pp. 26–36, 2018.